Development 126, 2299-2307 (1999)
Printed in Great Britain © The Company of Biologists Limited 1999
DEV7713

Drosophila embryonic pattern repair: how embryos respond to cyclin E-induced ectopic division

Qian-Jun Li*, Todd M. Pazdera and Jonathan S. Minden‡

Department of Biological Sciences and the Center for Light Microscope Imaging and Biotechnology, Carnegie Mellon University, Pittsburgh, PA 15213, USA

*****Present address: Pacific Agricultural Research Center, Agriculture and Agri-Food Canada, Summerland, BC V0H 1Z0, Canada

‡Author of correspondence (e-mail: minden@cmu.edu)

Accepted 25 February; published on WWW 19 April 1999

SUMMARY

The *Drosophila melanogaster* embryo ordinarily undergoes thirteen cycles of rapid syncytial division followed by three rounds of cellular division for most cells. Strict regulation of the number of divisions is believed to be essential for normal patterning and development. To determine how the embryo responds to hyperplastic growth, we have examined epidermal development in embryos that experience additional rounds of mitosis as the result of ectopic Cyclin E expression. We observed that the cell density in the epidermis nearly doubled within 1 hour of Cyclin E induction. The spacing and width of the ENGRAILED and *wingless* stripes was unchanged, but the cell density within the stripes was increased. By 4 hours after Cyclin E induction, the cell density had returned to almost normal values. The embryos developed, albeit more slowly, to produce viable larvae and adults. The excess cells were removed by apoptosis in a *reaper*-dependent fashion as evidenced by increased *reaper* expression. Embryos lacking cell death in the abdomen exhibited changes in ENGRAILED expression. In addition, germband retraction and dorsal closure were slower than normal. Ectopic Cyclin E expression in cell-death-deficient embryos exacerbated the germband retraction and ENGRAILED-expression defects.

Key word: Cyclin E, Cell proliferation, Programmed cell death, Apoptosis, Compensation, *Drosophila*

INTRODUCTION

Establishment and maintenance of a proper pattern requires precise control of cell proliferation and cell death. In metazoans, cell death and cell multiplication must be balanced in order to maintain tissue architecture (Evan et al., 1995). In *Drosophila*, there is a wealth of information about the genes and mechanisms required for embryonic pattern formation (Martinez Arias, 1993; Technau and Campos-Ortega, 1986), but little is known about pattern maintenance and repair. Insects and amphibians have an impressive capacity to repair patterning mistakes. This was generally studied by observing regeneration in surgically altered tissue (Bryant et al., 1981; French et al., 1976) or by ultraviolet irradiation of insect imaginal discs and embryos (Yasuda et al., 1991; King and Bryant, 1982). The main limitation of these studies was the need for physical manipulation of individual embryos, which prevented the molecular analysis of the repair process.

In an effort to understand the molecular/genetic mechanisms of pattern repair, we have begun to analyze how genetically mispatterned embryos are repaired. Analysis of embryos laid by females with varying doses of the anterior morphogen gene, *bicoid* (*bcd*), showed that mispatterning along the anterior-posterior axis could be efficiently corrected (Frohnhöffer and Nüsslein-Volhard, 1986; Berleth et al., 1988; Driever and Nüsslein-Volhard, 1988; Namba et al., 1997). Increasing or decreasing the maternal *bcd* dosage led to an expansion or compression of the anterior fate map, respectively. These embryos were capable of repairing this mispatterning and produced mostly normal animals. Expanded regions of the fate map were repaired by eliminating excess cells through programmed cell death, or apoptosis (Namba et al., 1997); whereas compressed regions of the fate map did not appear to be repaired (Busturia and Lawrence, 1994; Namba et al., 1997).

bcd-induced mispatterning changes the proportion of cells fated to form different regions of the embryo, it does not alter the overall cell density of the embryo. Another form of mispatterning is cell overgrowth or hyperplasia. *Drosophila* embryogenesis can be coarsely divided into two stages: a 3 hour period of 13 rounds of rapid, syncytial nuclear division and a 21 hour period of cell differentiation and organogenesis. Most cells in this latter period experience three rounds of mitosis in the 3 hours following the completion of cellularization, which separates the two phases. Neuronal precursors experience many more divisions; amnioserosa cells do not divide after cellularization (Hartenstein and Campos-Ortega, 1985; Foe, 1989). After the sixteenth division, most cells arrest at G_1 of cycle 17 (Campos-Ortega and Hartenstein, 1985; Bate and Martinez Arias, 1991). In an effort to drive cells

through an additional round of mitosis, we relied on the observation that ectopic expression of *DmcycE* shortly after the final mitosis bypasses the normal G_1 arrest and induces progression through an additional cell cycle in most epidermal cells (Richardson et al., 1993; Knoblich et al., 1994).

While most studies on the ectopic expression of *DmcycE* have focused on the molecular aspects of the extra cell division, little is known about the fate of the additional cells. In the eye imaginal disc, ectopic expression of *DmcycE* was shown to induce premature entry into the S phase, which led to the mispatterning of the adult eye by altering the number of photoreceptor cells per ommatidium and the development of the surrounding cells (Richardson et al., 1995). Mispatterning was not observed in all individuals and the roughening of the eye was not very severe, indicating that the initial mispatterning was repaired. We have employed *hs-DmcycE* embryos as a model for studying how embryos deal with a global increase in cell density. Using three-dimensional, time-lapse microscopy to monitor cell division and programmed cell death, we show here that *DmcycE*-induced excess cells were removed by apoptosis in a *reaper*-dependent manner and that the embryos survived to form mostly normal larvae. Increased cell density within the expression domains of the segment polarity genes, *engrailed (en)* and *wingless (wg)*, was observed 1 hour after *hs-DmcycE* induction, but was normalized within 4 hours of induction. Embryos that were deficient for cell death had altered EN stripe patterns and defective head involution, germband retraction and dorsal closure. All of these defects were more severe in cell-death-deficient embryos with ectopically expressed *hs-DmcycE*.

MATERIALS AND METHODS

Fly strains

Oregon-R was used as the wild-type stock. A stock that carried type I *DmcycE* cDNA under the control of the heat-shock promoter (*hs-DmcycE*) was provided by Dr H. Richardson (Richardson et al., 1995). The *P* element that carried *hs-DmcycE* was located on the third chromosome of this homozygous viable stock. *Df(3)H99/TM3*, referred to as *H99*, was used to generate cell-death-deficient embryos (provided by Dr H. Steller). *Df(3)W4/TM3*, which overlaps the *H99* deletion, was provided by the Bloomington Stock Center. A stock that carried *P[hs-DmcycE]* insertion and the *H99* deficiency was made by recombination. This stock will be referred to as *H99, hs-DmcycE*. Flies were grown on standard fly media at 25°C (Ashburner, 1989).

Induction of *DmcycE* gene expression

Heat-shock induction was performed as follows: embryos collected over a 1 hour interval were incubated at 25°C until they reached late stage 11 or early stage 12. The embryos were shifted to 37°C by either submerging the egg collection plate in a temperature-controlled water bath for 30 minutes or the embryos were heat shocked in large batches by washing into a 200 ml beaker with prewarmed, 37°C egg-wash solution that contained 0.04% Triton X-100 and 0.12 M NaCl, incubated for 35 minutes at 37°C, strained and washed with 25°C egg-wash solution. After heat shock, the embryos were returned to 25°C and aged for 1, 2 or 4 hours. Alternatively, embryos were prepared for microinjection and time-lapse microscopy by mounting on microscope coverslips according to Minden et al. (1989). The embryos on the microscope coverslips were heat shocked at the desired stage on the temperature-controlled block of a PCR thermocycler (Perkin-Elmer). All three methods of heat shocking gave essentially the same results.

Cuticle preparation

First instar larvae cuticles were prepared according to Lamka et al. (1992) and analyzed using phase-contrast or dark-field microscopy.

Cell density measurement

To measure epidermal cell density, embryos at the desired stage were fixed according to Namba et al. (1997) and mechanically devitellinized by vigorous shaking in 1:1 heptane:80% MeOH in PBS. The embryos were washed three times for 10 minutes each in PBT buffer (PBS plus 0.3% Triton X-100) at room temperature and then treated with RNase (10 μg/ml, Boehringer Mannheim) for 3 hours in 37°C. The digestion was stopped by the addition of EGTA to a final concentration of 2.5 mM. The embryos were then washed repeatedly every 10 minutes with PBT. Nuclear DNA was stained with 0.1 μg/ml propidium iodide (Sigma). After extensively washing the embryos with PBT, they were mounted in 50% glycerol and imaged by confocal microscopy using a 60× objective lens (MRC-600, Bio-Rad). Five optical sections of the dorsolateral region, taken 2 μm apart, were recorded for each embryo. The cell density in the epidermis was determined by counting the number of nuclei at the surface of the embryo in a 21.9×21.9 μm square area in the dorsolateral region of segments A3 and A4. Image analysis was performed on a Silicon Graphics workstation using DeltaVision 1.20 software (Applied Precision, Issaqua, WA).

Gross embryonic development

To analyze gross embryonic development, transmitted-light, time-lapse recordings were taken at 5 minute intervals according to Minden et al. (1989). The development of up to 20 embryos per session was recorded using a programmable stage that repeatedly cycled between embryos.

Monitoring cell death and mitosis in vivo

Three-dimensional, time-lapse recording of cell death and mitosis was performed according to Namba et al. (1997). To monitor the mitotic activity, postcellularization stage embryos were injected with 1.5 mM RGPEG into intervitelline space (Minden, 1996). To monitor the programmed cell death, Acridine orange (AO) at 0.5 mg/ml in PBS was injected into the cytoplasm of precellularization stage embryos. Each recording consisted of multiple time points taken at 5 minute intervals; each time point consisted of a stack of the six optical sections taken 5 μm apart. The time-lapse recordings were processed and analyzed using DeltaVision 1.20 software.

Quantification of cell death

The number of dying cells was determined by counting AO-positive nuclei from projected image stacks selected at 50 minutes intervals from the time-lapse recordings. The 50 minute interval was used to ensure the dying cells were not counted twice since it takes 30-45 minutes for AO-positive cells to be removed by macrophages or neighboring cells. Cell death counting was restricted to the germband epidermis; the fluorescent signals from yolk autofluorescence and amnioserosa were excluded. The fluorescent signal originating in macrophages, which appeared as large nuclei containing multiple fluorescent bodies, was also ignored.

In situ hybridization

In situ hybridization was performed according to Tautz and Pfeifle (1989). The *reaper (rpr)* DNA probe was generated according to Namba et al. (1997). The *wg* probe was generated by cutting *wg* cDNA (provided by Dr R. Nusse) with *Bam*HI and *Pvu*I. Probes were labeled with digoxigenin-dUTP by Klenow fragment and detected according the protocol provided by the DIG DNA labeling and detecting kit (Boehringer Mannheim). To double label for *wg* expression and cell density, dehydrated *wg* in situ-stained embryos were rehydrated in PBT and stained with propidium iodide as described above. The embryos were washed in PBT, dehydrated in

ethanol, then stepped into 100% xylene and mounted in xylene:permount. The embryos were imaged with confocal microscopy using a 40× objective lens and rhodamine filter set (MRC-600, Bio-Rad).

Antibody staining

Antibody staining was performed according to Bomze and Lopez (1994). Anti-EN monoclonal antibody (provided by Dr T. Kornberg) was used at a 1:1000 dilution in 1% BSN. Horse anti-mouse IgG served as secondary antibody at a 1:1000 dilution and immunostains were performed according to Vectastain Elite ABC kit (Vector Laboratory).

RESULTS

Gross development and cuticle pattern in *hs-DmcycE* embryos

Ectopic expression of *DmcycE* during stage 11 or early stage 12 drives most epidermal cells through an extra round of cell division as shown by BrdU incorporation and anti-tubulin antibody staining (Knoblich et al. 1994). Since we were interested in the dynamics of how the embryo responds to excess cell division, we used a number of time-lapse microscopy methods to analyze heat-shocked wild-type and *hs-DmcycE* embryos. Time-lapse, three-dimensional, fluorescence microscopy of *hs-DmcycE* embryos injected with a fluorescent dye, RGPEG, into the intervitelline space revealed a single, ectopic round of cell division, which occurred within 1 hour after applying a heat shock in early stage 12 (data not shown). To analyze the gross development of *hs-DmcycE* embryos after heat shock, time-lapse, transmitted-light recordings were made. Both heat-shocked wild-type and *hs-DmcycE* embryos started germband retraction normally, but the *hs-DmcycE* embryos required approximately 30 minutes longer to complete retraction. The duration of germband retraction in wild-type embryos is typically 2 hours at 25°C. Clusters of cells were often seen floating in the intervitelline space above the amnioserosa of *hs-DmcycE* embryos; this was not seen in wild-type embryos (Fig. 1A,B). After germband retraction, *hs-DmcycE* embryos continued to develop normally, but more slowly than wild type (Fig. 1D). 83% of wild-type embryos hatched within 24 hours of heat shock at stage 12. This value plateaued at 91% by 48 hours after heat shock. In comparison, only 15% *hs-DmcycE* embryos hatched within 24 hours of heat shock. The percentage of hatched embryos increased to 54% by 36 hours after heat shock and reached a maximum level of 65% by 48 hours after heat shock. One-quarter of the hatched, heat-shocked *hs-DmcycE* embryos reached adulthood. The *hs-DmcycE* embryos that failed to hatch were defective in germband retraction and epidermal integrity as seen by yolk leaking into the intervitelline space (data not shown).

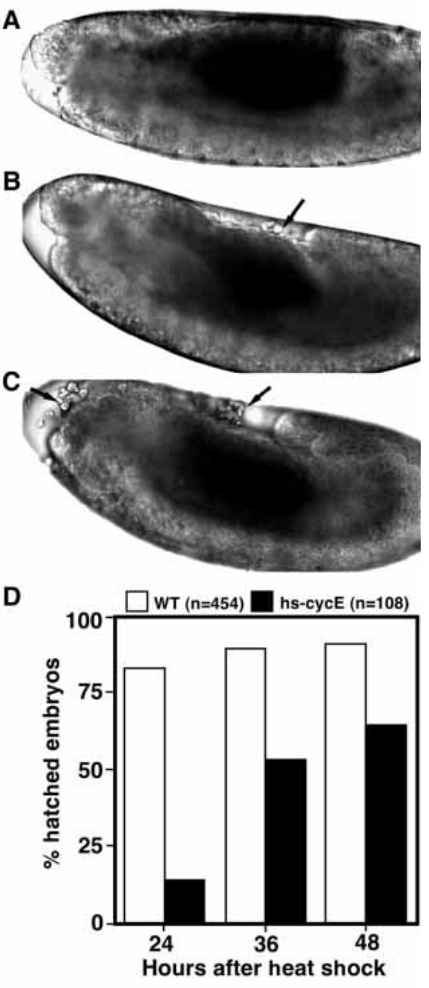

Fig. 1. The gross development of wild-type, *hs-DmcycE* and *H99, hs-DmcycE* embryos. Images were selected from the transmitted-light, time-lapse recordings. (A) An early stage 13 wild-type embryo 2 hours after heat shock, the germband has completely retracted. (B) A late stage 12 *hs-DmcycE* embryo 2 hours after heat shock, the germband is mostly retracted. (C) A mid-stage 12 *H99, hs-DmcycE* embryo 4 hours after heat shock, the germ band is only half retracted. The arrows in B and C indicate groups of cells floating in the intervitelline space adjacent to the amnioserosa and head. (D) Shows a bar graph of the percentage of embryos that hatched by the indicated times after a heat shock was applied at stage 12.

In order to assess the effect of extra mitoses on epidermal patterning, the cuticle of heat-shocked *hs-DmcycE* embryos was compared to heat-shocked wild-type embryos. *hs-DmcycE* embryos that hatched displayed no overt cuticle defects (data not shown). However, close examination of denticle belts A3 and A4 revealed an approximately 14% increase in the number of denticle hairs per segment. This increase was graded within each denticle belt where the first and second rows had 34% and 23% more denticles, respectively (Table 1; Fig. 2A,B). The increase in the third row was 11%; while the combined fourth and fifth rows increased 6%. The increased denticle number resulted in wider rows and closer denticle spacing.

Table 1. The number of denticle hairs in segments A3 and A4 of heat-shocked wild-type and *hs-DmcycE* embryos

		Denticle number in different rows			
Segment	Embryo type	1	2	3	4+5
A3	WT	29.6±1.9	14.9±0.5	24.6±3.7	71.2±5.7
	hs-DmcycE	40.7±5.6	17.8±1.8	26.9±2.5	78.0±3.9
A4	WT	28.2±2.5	14.3±1.0	23.3±1.5	75.8±2.9
	hs-DmcycE	36.8±3.8	18.2±2.5	26.3±3.2	77.7±5.0
% increase versus wild type		34%	23%	11%	6%

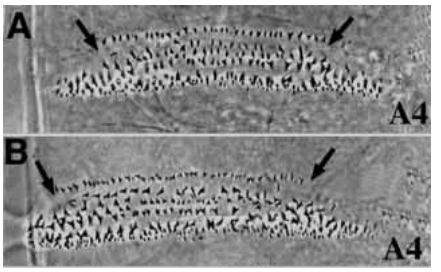

Fig. 2. Cuticle analysis of first instar larvae. (A) The denticle pattern in the A4 segment of a wild-type embryo. (B) The denticle pattern in the A4 segment of heat-shocked *hs-DmcycE* embryo. Anterior is up. The arrows indicate the width of the first row of denticles.

Fluctuation of cell density in *hs-DmcycE* embryos

Since the epidermal cells experienced an addition round of mitosis during stage 12 and the cuticle pattern was mostly normal by stage 17, we decided to measure epidermal cell density at various times after heat-shock induction of *hs-DmcycE* in comparison to wild-type embryos. The protocol was to heat shock embryos at early stage 12 and determine the cell density at 1, 2 and 4 hours post-heat shock. The number of propidium iodide-stained, epidermal-cell nuclei was determined in a 21.9×21.9 μm area in the dorsolateral region of segments A3 and A4 midway between the segment borders (Fig. 3A). This area will be referred to as the unit area. Since there was very little difference in cell density between A3 and A4, the values presented are the average cell density of both segments for five to ten embryos for each time point. As a baseline, both *hs-DmcycE* and wild-type embryos had cell densities of 30 cells/unit area at early stage 12 without heat shock. For wild-type embryos, the cell density decreased to 24 cells/unit area 1 hour after heat shock and remained constant over the next several hours. For *hs-DmcycE* embryos, the cell density increased to 38 cells/unit area, a 62% increase over wild type, 1 hour after heat shock. The cell density of heat-shocked, *hs-DmcycE* embryos decreased over the next several hours. By 2 hours after heat shock, the cell density decreased to 57% above wild type and, by 4 hours, the cell density was 18% above normal. This increase in cell density was also observed in first instar larvae (data not shown).

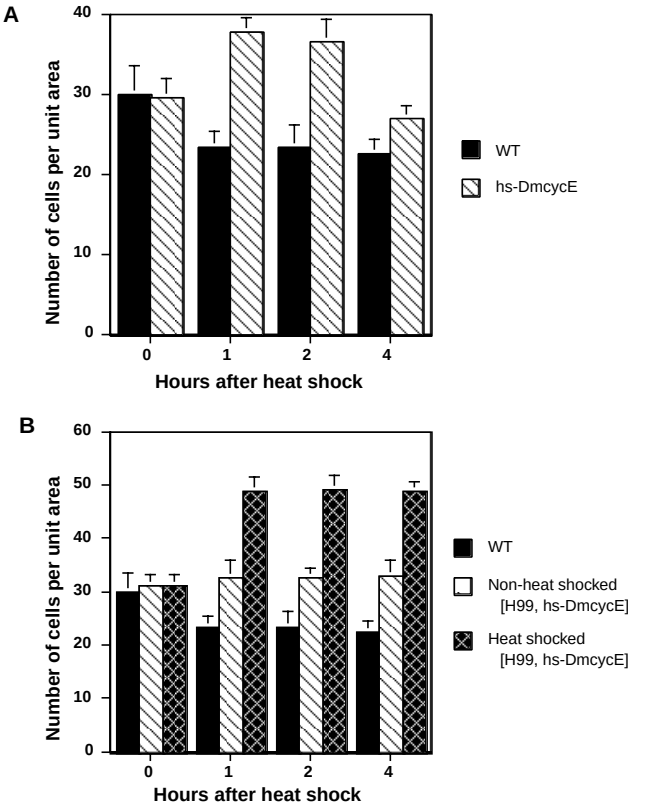

Fig. 3. Cell density changes in the epidermis of wild-type, *hs-DmcycE*, *H99* and *H99, hs-DmcycE* embryos. (A) A graph of cell density of wild-type and *hs-DmcycE* embryos at various times after heat shock at stage 12. (B) A graph of cell density of wild-type and *H99, hs-DmcycE* embryos that were heat shocked at stage 12 and non-heat-shocked *H99, hs-DmcycE* embryos at various times after stage 12.

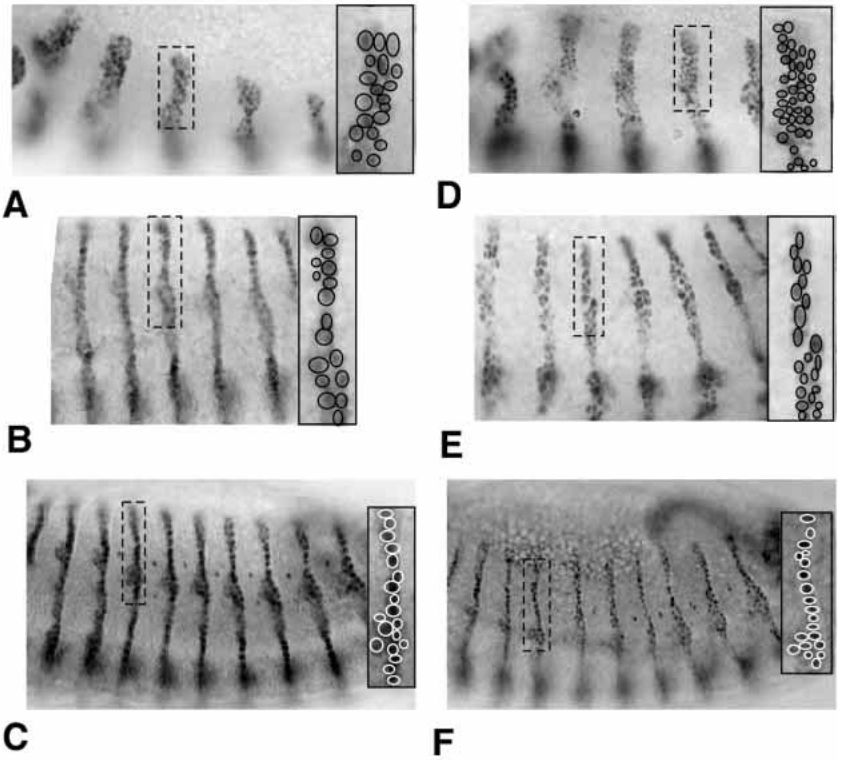

Fig. 4. Dynamic changes of *en* expression after ectopic expression of *hs-DmcycE*. Anti-EN antibody was used to monitor the changes in *en* expression in wild-type and *hs-DmcycE* embryos at various times after a stage 12 heat shock. (A) and (D) Wild-type and *hs-DmcycE* embryos 1 hour after heat shock, respectively. (B) and (E) Wild-type and *hs-DmcycE* embryos 2 hours after heat shock, respectively. (C) and (F) Wild-type and *hs-DmcycE* embryos 4 hours after heat shock, respectively. The area inside the dashed boxes are magnified in the inserts. Individual nuclei are highlighted with black or white ovals.

The expression pattern of *en* and *wg*

To assess the effect of extra mitoses on epidermal patterning, the expression of the segment polarity genes, *en* and *wg*, was examined in heat-shocked wild-type and *hs-DmcycE* embryos. Anti-EN antibody staining revealed an approximately 1.5-fold increase of cell density within the *en* stripe 1 hour after heat shock (compare Fig. 4A and D). The absolute width and spacing of the stripes was unchanged relative to wild type at the same developmental stage. The cells within the *en* stripe of heat-shocked *hs-DmcycE* embryos appeared to be smaller in cross section than wild-type cells. The *en* stripe normalized very rapidly. By 2 hours after heat shock, the cell density of the stripe was still greater than wild type, but not as dense as the 1 hour time point. The nuclei appeared to regain their normal size, but some were irregularly shaped. By 4 hours after heat shock, the cell density within the *en* stripe was only slightly increased over wild type (Fig. 4B,E,C and F).

hs-DmcycE embryos probed for *wg* mRNA expression displayed a similar increase of cell density within the *wg* stripe 1 hour after heat shock (compare Fig. 5A and B). It was difficult to count the number of *wg*-expressing cells due to the diffuse hybridization pattern. To circumvent this limitation, the embryos were also labeled with propidium iodide to visualize all nuclei. The *wg*-expressing cells appear as darkened patches against the bright background of fluorescent nuclei. The area of *wg* expression was not increased, only the number of *wg*-expressing cells was increased. To ensure that the changes in cell density were not an artefact of the heat-shock protocol, three different methods of heat shock were used. In all cases, the results were the essentially the same. The re-establishment of the normal *wg* pattern appeared to be slightly slower than the correction of the *en* pattern. The cell density within the *wg* expression domains remained more elevated 2 hours after heat shock, but was close to normal by 4 hours after heat shock (Fig. 5). These data indicate that the *DmcycE*-induced cell density increase was rapidly repaired and that normal *en/wg* patterning was re-established with similar dynamics.

Removal of extra cells by programmed cell death

The fluctuation of cell density and re-establishment of the segment polarity gene expression patterns in *hs-DmcycE* embryos 4 hours after heat shock and the appearance of free-floating cells in the intervitelline space suggested that the heat-shocked *hs-DmcycE* embryos eliminated massive numbers of cells in a very short period, possibly by programmed cell death. Two approaches were taken to examine programmed cell death: three-dimensional, time-lapse microscopy of AO-injected embryos to determine cell death dynamics and in situ detection of *rpr* gene expression in fixed embryos (White et al., 1994; Namba et al., 1997). Previous analysis of cell death dynamics in *Drosophila* embryos using AO showed that the nuclei of dying cells become highly fluorescent. The fluorescent signal from a dying cell persisted for 30-45 minutes and was then extinguished due to engulfment of the dead cell by scavenging macrophages or neighboring cells (Abrams et al., 1993; Namba et al., 1997; Pazdera et al., 1998). Selected time points from time-lapse recordings of wild-type and *hs-DmcycE* embryos that were injected with AO and heat-shocked at stage 12 are shown in Fig. 6. To quantify the dying cells in the germband epidermis, images were projected, deconvolved and spot detected (Namba et al., 1997; Pazdera et al., 1998). The number of dying cells from stage 12 to 14 was counted by summing cell death figures over 6 time points taken at 50 minute intervals. This ensured that each dying cell was only counted once. In wild-type embryos, cell death was first detected at late stage 11 at the tip of the germband, where a group of cells died at the beginning of the germband retraction. Afterwards, cell death became more widespread and prominent

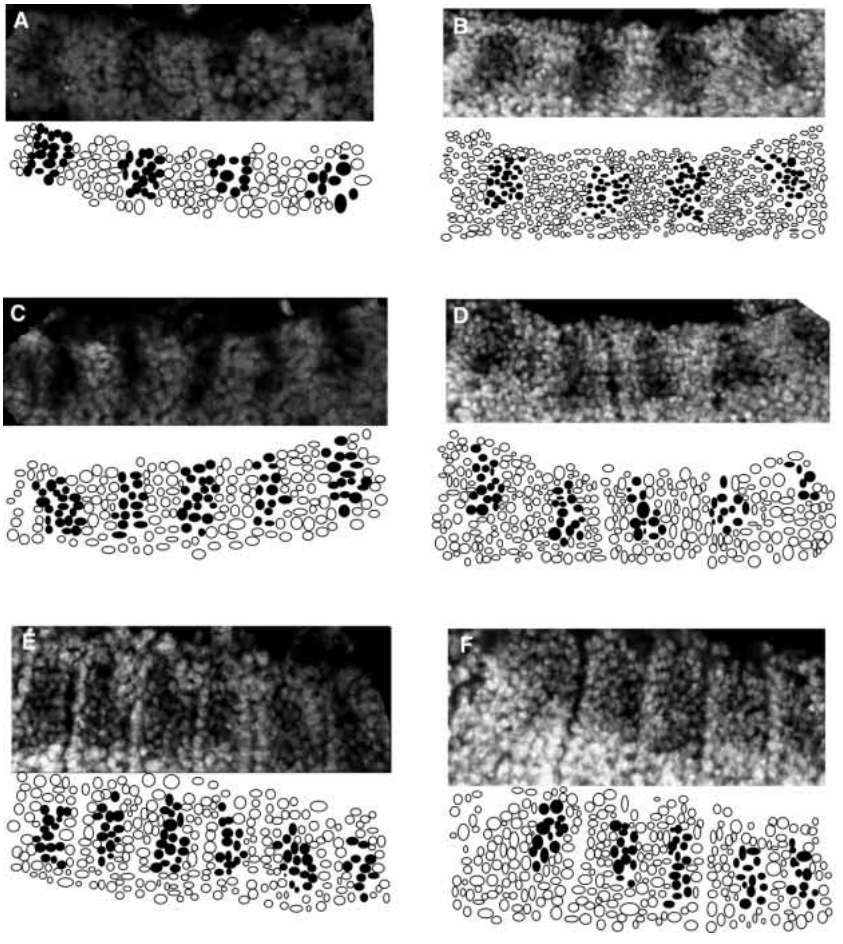

Fig. 5. Dynamic changes of *wg* expression after ectopic expression of *hs-DmcycE*. In situ hybridization was used to monitor the changes in *wg* expression in wild-type and *hs-DmcycE* embryos at various times after heat shock. Wild-type (A) and *hs-DmcycE* (B) embryos 1 hour after heat shock. Wild-type (C) and *hs-DmcycE* (D) embryos 2 hours after heat shock. Wild-type (E) and *hs-DmcycE* (F) embryos 4 hours after heat shock, respectively. All nuclei were stained with propidium iodide. Regions of wg expression appear as darkened areas. Below each fluorescent image is a cartoon of the nuclei. The black ovals represent *wg*-expressing nuclei; the white ovals are nuclei that not express *wg*.

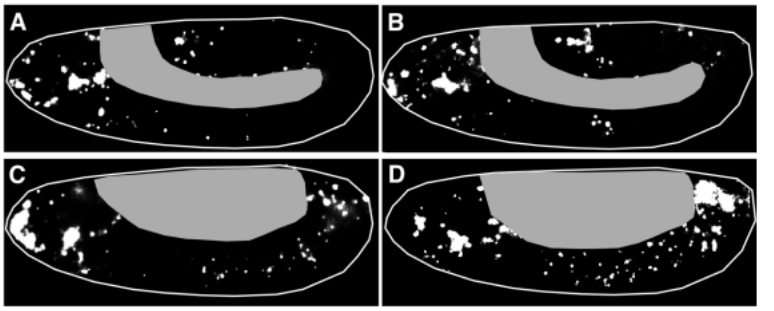

Fig. 6. Cell death in wild-type and *hs-DmcycE* embryos. Shown here are selected images from time-lapse recordings of embryos injected with Acridine orange. (A) and (B) Wild-type and *hs-DmcycE* embryos at the middle of stage 12, respectively. (C) and (D) Wild-type and *hs-DmcycE* embryos at early stage 14, respectively. Newly dying cells appear as small AO-positive spots. Macrophages that have engulfed dying cells appear as large irregular spots. The fluorescent signal from the amnioserosa and yolk were masked by the grey shading.

particularly in the ventrolateral epidermis. Between stage 12 and 14, about 140 cells died over the entire length of the germband in the lateral epidermis of wild-type embryos. In heat-shocked *hs-DmcycE* embryos, the pattern of cell death was initially very similar to the wild-type cell death pattern. However, at the completion of germband retraction, there was a large increase in cell death. The increase of cell death in each segment first appeared adjacent to the segment borders and then spread into the middle of the segment. The temporal pattern of ectopic cell death could explain why the cell density appeared to decrease more rapidly in the *en*-expressing cells, which lie at the posterior border of each segment, than the *wg*-expressing cells, which are located near the middle of the segment. The number of cell deaths increased three-fold to 430 cell deaths over the same developmental period.

To examine whether the additional cell deaths were the result of *rpr*-dependent apoptosis, heat-shocked wild-type and *hs-DmcycE* embryos were fixed and probed for *rpr* mRNA expression. In both wild-type and *hs-DmcycE* embryos, *rpr* expression was first detected at stage 10 in a diffuse and somewhat segmented pattern (Namba et al., 1997; Pazdera et al., 1998). The *rpr*-expression pattern became more restricted over time to highlight individual cells at stage 13 (data not shown). This later pattern was similar to the AO-fluorescence pattern. Comparison of embryos 3 hours after heat shock showed a large increase in *rpr*-positive cells in *hs-DmcycE* embryos (data not shown). Cells expressing *rpr* in *hs-DmcycE* embryos were smaller than those in wild-type embryos, indicating that the dying cells had undergone an additional mitosis. These data indicate that the mechanism for removal of *DmcycE*-induced extra cells is mediated by *rpr*-dependent apoptosis.

Cell-death-deficient embryos are unable to repair hyperplastic defects

Since programmed cell death plays the key role in removing excess cells in heat-shocked *hs-DmcycE* embryos, we were interested in determining the effect of eliminating cell death genes in heat-shocked *hs-DmcycE* embryos. The deficiency stock, *H99*, deletes three major *Drosophila* cell death genes, *rpr, hid* and *grim*, which lie within a small interval on the left arm of the third chromosome (White et al., 1994). A recombinant stock that carried both the *H99* deficiency and *P[hs-DmcycE]* was generated (referred to as *H99, hs-DmcycE*). Several methods were used to discriminate between homozygous *H99, hs-DmcycE* embryos and *H99/TM3* or *TM3/TM3* embryos: (1) failure to detect in vivo *ftz-lacZ* expression arising from a TM3 balancer chromosome that carried a *ftz-lacZ* marker as detected by RGPEG injection (Minden 1996), (2) failure to detect AO-positive cells in vivo, (3) failure to detect *rpr* mRNA in fixed embryos and (4) the appearance of head involution defects in fixed embryos. Heat-shocked homozygous *H99, hs-DmcycE* embryos developed more abnormally than the heat-shocked parental *H99* and *hs-DmcycE* stocks. *H99* embryos had a mild germband retraction defect; heat-shocked *hs-DmcycE* embryos had slightly delayed germband retraction; while heat-shocked *H99, hs-DmcycE* embryos had a much more severe germband retraction defect. In addition, the number of free-floating cells in the intervitelline space and the frequency of yolk leakage was greatly increased in heat-shocked *H99, hs-DmcycE* embryos compared to heat-shocked *hs-DmcycE* embryos (Fig. 1C).

Homozygous *H99, hs-DmcycE* embryos that were not heat shocked, had a cell density that was initially the same as wild type at early stage 12, but increased to 42% above wild type 1 hour into stage 12 and remained at this level for several hours (Fig. 3B). The cell density in *H99, hs-DmcycE* embryos that were heat shocked at the start of stage 12 increased to twice wild type within 1 hour of heat shock and remained constant over several hours (Fig. 3B).

Examination of the *en* stripes in homozygous *H99* embryos at stage 13 revealed that the stripes were wider than normal at some positions along the dorsoventral axis and completely absent at other positions. In addition, the level of *en* expression appeared more variable (compare Fig. 7A and B). The *en* pattern in *H99* embryos was the same with and without heat shock. Similar defects as those observed for *H99* homozygous embryos were observed for *H99/Df(3)W4* transheterozygotes, which have overlapping deletions (data not shown). *H99, hs-DmcycE* embryos that were heat shocked at the start of stage 12 showed a similar expansion of the *en* stripe as their *hs-DmcycE* counterparts (data not shown). 3 hours after heat shock, when the embryos should have been in stage 13, the *en* stripes partially narrowed and became discontinuous and disorganized (Fig. 7C). This embryo appears to be in the middle of stage 12 because of its germband retraction defect. Ordinarily, there is a single *en*-expressing cell in the middle of each segment (Fig. 7A insert); however, in *H99* and heat-shocked *H99, hs-DmcycE* embryos multiple *en*-expressing cells were observed (Fig. 7B and C inserts). This was more pronounced in the heat-shocked *H99, hs-DmcycE* embryos.

DISCUSSION

Morphogenetic effects of an extra cell division

Previous analysis of heat-shocked *hs-DmcycE* embryos

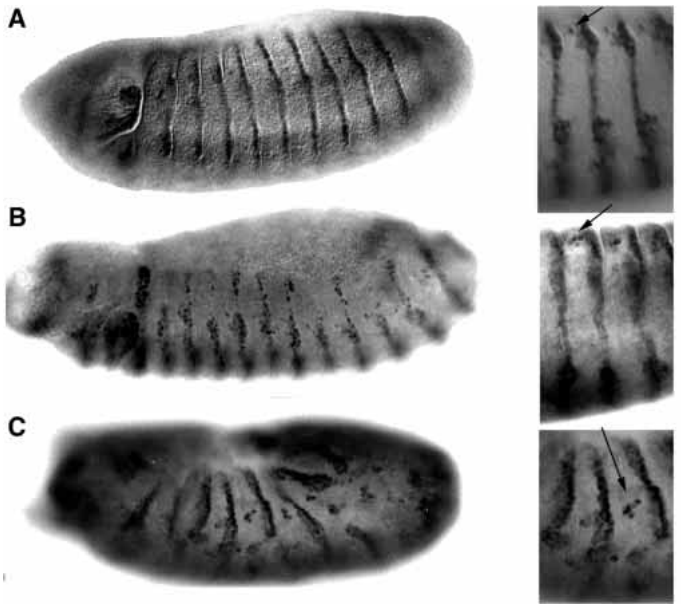

Fig. 7. *en* expression in *H99* and *H99, hs-DmcycE* embryos. Anti-EN antibody was used to monitor *en* expression in fixed embryos at various times with and without heat-shock treatment. (A) A wild-type embryo at stage 13. (B) A homozygous *H99* embryo at stage 13. (C) A homozygous *H99, hs-DmcycE* embryo 3 hours after heat shock at stage 13. The left of each panel shows a higher magnification view of the mid-segment *en*-expressing cell(s) as indicated by the arrow.

demonstrated that *DmcycE* mRNA was detectable in all cells soon after induction (Sauer et al., 1995), epidermal cells entered S phase within 20 or 120 minutes when heat shocked at stage 11 or 12, respectively, that resulted in an extra round of cell division (Knoblich et al., 1994). In vivo monitoring of mitosis by intervitelline injection of a fluorescent dye confirmed these results showing that the ectopic divisions in the epidermis occurred within 30 minutes of *hs-DmcycE* induction in early stage 12 embryos (data not shown). There is an apparent difference in the dynamics of the ectopic cell division reported here and by Knoblich et al. (1994). This difference is probably the result of slight differences in the stage at which the heat shock was applied, the method for applying the heat shock and incubation conditions. The cell density reached a maximum level 1 hour after heat shock. Since all of the epidermal cells in heat-shocked *hs-DmcycE* embryos appeared to have undergone an additional mitosis, one would expect a 100% increase in cell density, but the observed increase was only 62%. A similar increase in cell density has been reported in embryos that are mutant for the cyclin-dependent kinase inhibitor, *dacapo*, which causes a 45-70% increase in cell density in the epidermis at stage 14 (Lane et al., 1996; de Nooij et al., 1996). One possible explanation for the observed less than two-fold increase in cell density is that cell death, which starts at late stage 11, may have begun to remove the excess cells. This is supported by the doubling of cell density in heat-shocked *H99, hs-DmcycE* embryos 1 hour after *DmcycE* induction (Fig. 3B). It is not clear if *dacapo* mutant embryos are capable of repairing the increased cell density, nor is it known if *dacapo* embryos experience only a single ectopic round of cell division.

There were three prominent morphogenetic defects caused by the excess cells in heat-shocked *hs-DmcycE* embryos: difficulty in germband retraction, the appearance of free-floating cells in the intervitelline space and delayed development. Germband retraction is a poorly understood process. There are a number of genes that affect germband retraction: *hindsight*, *serpent*, *tailup* and *u-shaped* (Nüsslein-Volhard et al., 1984; Wieschaus et al., 1984). Homozygous *H99* embryos had mild germband retraction defects, while heat-shocked *H99, hs-DmcycE* embryos were severely defective. Time-lapse recordings of heat-shocked *H99, hs-DmcycE* embryos showed that the germband initially attempted to retract, but the progress was impeded. The time-lapse recordings of intervitelline injected *hs-DmcycE* embryos showed that some of the amnioserosa cells also experienced ectopic divisions, which may have interfered with germband retraction. The germband retraction defect in *hs-DmcycE* embryos may simply be the result of steric hindrance caused by the increased cell number in both the germband and amnioserosa.

During the phase when the germband is attempting to retract, a large number of free-floating cells spilled into the intervitelline space both at the amnioserosa and the anterior tip of the embryo in heat-shocked *H99, hs-DmcycE* embryos. This was also seen in heat-shocked *hs-DmcycE* embryos, but to a lesser extent. Clusters of intervitelline cells have been seen previously in 6*bcd* embryos at the same stage of development (Namba et al., 1997). All of these embryos were attempting to repair expanded tissues. The origin of the intervitelline cells is not yet clear. An early event in apoptosis is the loss of contact between the dying cell and its neighbors. If a large patch of cells died simultaneously, cells in the middle of the patch may be discharged into the intervitelline space as a cluster or may cause a tear in the epithelium allowing cells beneath the epithelium to escape into the intervitelline space. It is intriguing that heat-shocked *H99, hs-DmcycE* embryos, which were unable to initiate *rpr*-dependent apoptosis, still had the same cell loss phenotype. This indicates that the signal for loss of cell-cell contact during programmed cell death may be upstream or independent of *rpr, hid* and *grim*.

The majority of heat-shocked *hs-DmcycE* embryos required an additional 12 to 24 hours to hatch. The reason for this delay is not yet known. The data presented here indicate that the majority of excess epidermal cells were removed within 4 hours of heat shock and that germband retraction was only delayed by 30 minutes. Presumably other embryonic tissues were affected by ectopic *hs-DmcycE* expression which required extra time to repair these affected tissues. One indication of other tissues undergoing ectopic divisions was a dramatic increase in *rpr* expression in the procephalic region of heat-shocked *hs-DmcycE* embryos (data not shown).

Re-establishment of normal segment polarity gene expression is a component of pattern repair

Patterning in the epidermis depends on the interactions between *wg*- and *en*-expressing cells. Altering the expression of these genes or components of their respective signaling pathways alters the epidermal patterning. The extra cell divisions in the epidermis caused increased cell density of both

en and *wg* expression stripes, but did not affect their width or spacing. The *en* stripe was repaired within 2 hours of *hs-DmcycE* induction; the *wg* stripe was repaired within 4 hours of induction. The repair of the *en* stripe was not complete as evidenced by the increased number of first row denticles, which are dependent on *en* expression. Mapping epidermal cell death in wild-type embryos revealed that *wg*-expressing and responding cells in the middle of the segment experienced less cell death than cells at the segmental borders (Pazdera et al., 1998). Time-lapse recordings of cell death in heat-shocked *hs-DmcycE* embryos revealed a segmentally repeated pattern where cells at the segment borders were the first to die followed by the cells in the middle of the segment. This was confirmed by the pattern of *rpr* expression 3 hours after *hs-DmcycE* induction, which highlighted the cells in the middle segment indicating their impending death. These data indicate that the excess cells are removed in a pattern-specific fashion, not randomly.

What happens to cells that are destined to die, but are prevented from doing so by a mutation in the cell death pathway? Normally, *en* is expressed in a continuous stripe of cells. In *H99* and non-heat-shocked homozygous *H99*, *hs-DmcycE* embryos, the stripe of *en* expression became variable and discontinuous. The variability and discontinuity was more pronounced in heat-shocked homozygous *H99*, *hs-DmcycE* embryos. Apoptosis is believed to remove cells that are redundant and that are no longer useful. The variable expression and discontinuities in the *en* stripe may indicate cells that were destined to die and were turning off or had turned off *en* expression. Because the embryos were defective for cell death, the doomed cells remained in place creating gaps in the *en* stripe. Further experimentation is required to show that the cells in the gaps once expressed *en*. The appearance of these gaps may also be an indicator of events that are upstream or independent of *rpr*-, *hid*- and *grim*-associated cell death.

Conclusions

In order for a multicellular organism to develop, it must control the numbers and relative proportion of cells fated to generate a complete body. This process can be divided into two phases: establishment and maintenance. While there is a great deal known about the establishment of the body plan, we are only beginning to study tissue maintenance and the repair of developmental defects. We have previously shown that *Drosophila* embryos are capable of repairing disproportionately enlarged tissue by orchestrating the programmed cell death of the excess cells. The converse does not appear to be true; disproportionately reduced tissue is not repaired by increased cell division (Busturia and Lawrence, 1994; Namba et al., 1997). Here we show that embryos with increased cell density, but normal overall proportioning, are also capable of removing the excess cell by apoptosis. It is not yet clear how the embryo determines which cells are in excess and selected to die. The study of pattern repair is still in a phenomenological phase. We need a better understanding of the triggers and limits of pattern repair before the underlying mechanism can be determined.

We would like to thank Brian McNally for technical support. T. P. was supported in part by an NSF graduate training grant to the Science and Technology Center for Light Microscope Imaging and Biotechnology, BIR 9256343. J. M. is a Lucille P. Markey Scholar, and this work was supported in part by grants from the Lucille P. Markey Charitable Trust and NIH grant HD31642.

REFERENCES

Abrams, J. M., White, K., Fessler, L. I. and Steller, H. (1993). Programmed cell death during *Drosophila* embryogenesis. *Development* **117**, 29-43.

Ashburner, M. (1989). *Drosophila, a Laboratory Manual*. Cold Spring Harbor Laboratory Press.

Bate, M. and Martinez Arias, A. (1991) The embryonic origin of imaginal disc in *Drosophila*. *Development* **112**, 755-761.

Berleth, T., Burri, M., Thoma, G., Bopp, D., Richstein, S., Frigerio, G., Noll, M., and Nüsslein-Volhard, C. (1988). The role of localization of *bicoid* RNA in organizing the anterior pattern of *Drosophila* embryo. *EMBO J.* **7**, 1749-1756.

Bomze, H. M. and López, A. J. (1994). Evolutionary conservation of the structure and expression of alternatively spliced *ultrabithorax* isoforms from *Drosophila*. *Genetics* **136**, 965-977.

Bryant, S. V., French, V. and Bryant, P. J. (1981). Distal regeneration and symmetry. *Science* **212**, 993-1002.

Busturia, A. and Lawrence, P. A. (1994). Regulation of cell number in *Drosophila*. *Nature* **370**, 561-563.

Campos-Ortega, J. A. and Hartenstein, V. (1985). *The Embryonic Development of Drosophila melanogaster*. New York, Berlin, Heidelberg, Tokyo: Springer-Verlag.

de Nooij, J. C., Letendre, M. A. and Hariharan, I. K. (1996). A cyclin-dependent kinase inhibitor, *Dacapo*, is necessary for timely exit from the cell cycle during *Drosophila* embryogenesis. *Cell* **87**, 1237-1247.

Driever, W. and Nüsslein-Volhard, C. (1988). A gradient of BICOID protein in *Drosophila* embryos. *Cell* **54**, 83-93

Evan, G. I., Brown, L., Whyte, M. and Harrington, E. (1995). Apoptosis and the cell cycle. *Curr. Opin. Cell Biol.* **7**, 825-834.

Foe, V. E. (1989). Mitotic domains reveal early commitment of cells in *Drosophila* embryos. *Development* **107**, 1-22.

French, V., Bryant, S. V., and Bryant, P. J. (1976). Pattern regulation in epimorphic fields. *Science* **193**, 969-981.

Frohnhöffer, H. G. and Nüsslein-Volhard, C. (1986). Organization of anterior pattern in the *Drosophila* embryo by the maternal gene *bicoid*. *Nature* **324**, 120-125.

Hartenstein, V. and Campos-Ortega, J. A. (1985). Fate-mapping in wild-type *Drosophila melanogaster*. 1. The spatio-temporal pattern of embryonic cell divisions. *Rou's Arch. Dev. Biol.* **194**, 181-195.

King, B. H. and Bryant, P. J. (1982). Development response of the *Drosophila melanogaster* embryo to localized X irradiation. *Rad. Research* **89**, 590-606.

Knoblich, J. A., Sauer, K., Jones, L., Richardson, H., Saint, R. and Lehner, C. F. (1994). Cyclin E controls S phase progression and its down-regulation during *Drosophila* embryogenesis is required for the arrest of cell proliferation. *Cell* **77**, 107-120.

Lamka, M. L., Boulet, A. M. and Sakonlu, S. (1992). Ectopic expression of UBX and ABD-B proteins during *Drosophila* embryogenesis: competition, not a functional hierarchy, explains phenotypic suppression. *Development* **116**, 841-854.

Lane, M. E., Sauer, K., Wallace, K., Jan, Y. N., Lehner, C. F., and Vaessin, H. (1996). *Dacapo*, a cyclin-dependent kinase inhibitor, stop cell proliferation during *Drosophila* development. *Cell* **87**, 1225-1235.

Martinez Arias, A. (1993). Development and patterning of the larval epidermis of *Drosophila*. In *The Development of Drosophila melanogaster* (ed. Bate, M. And Martinez-Arias, A.), pp. 517-608. Cold Spring Harbor Laboratory Press.

Minden, J. S. (1996). Synthesis of a new substrate for detection of *lacZ* gene expression in live *Drosophila* embryos. *BioTechniques* **20**, 122-129.

Minden, J. S., Agard, D. A., Sedat, J. W. and Alberts, B. M. (1989). Direct cell lineage analysis in *Drosophila melanogaster* by time-lapse, three-dimension optical microscopy in living embryos. *J. Cell Biol.* **109**, 505-516.

Namba, R., Pazdera, T. M., Cerrone, R. L. and Minden, J. S. (1997). *Drosophila* embryonic pattern repair: how embryos respond to *bicoid* dosage alteration. *Development* **124**, 1393-1403.

Nüsslein-Volhard, C., Wieschaus, E. and Kluding, J. (1984). Mutations affecting the pattern of the larval cuticle in *Drosophila melanogaster*. I.

Zygotic loci on the second chromosome. *Wilhelm Roux's Arch. Dev. Biol.* **193**, 267-282.

Pazdera, T. M., Janardhan, P. and Minden, J. S. (1998). Patterned epidermal cell death in wild-type and segment polarity mutant *Drosophila* embryos. *Development* **125**, 3427-3436.

Richardson, H. E., O'Keefe, L. V., Reed, S. I. and Saint, R. (1993). A *Drosophila* G1-specific cyclin E homolog exhibits different modes of expression during embryogenesis. *Development* **119**, 673-690.

Richardson, H. E., O'Keefe, L. V., Marty, T. and Saint, R. (1995). Ectopic cyclin E expression induces premature entry into S phase and disrupts pattern formation in the *Drosophila* eye imaginal disc. *Development* **121**, 3371-3379.

Sauer, K., Knoblich, J. A., Richardson, H. and Lehner, C. F. (1995). Distinct modes of cyclin E/cdc2c kinase regulation and S-phase control in mitotic and endoreduplication cycles of *Drosophila* embryogenesis. *Genes Dev.* **9**, 1327-1339.

Tautz, D. and Pfeifle, C. (1989). A non-radioactive in situ hybridization method for the localization of specific RNAs in *Drosophila* embryos reveals translational control of the segmentation gene *hunchback. Chromosoma* **98**, 81-85.

Technau, G. M. and Campos-Ortega, J. A. (1986). Lineage analysis in embryos of *Drosophila melanogaster*. *Development* **100**, 1-12.

Wieschaus, E., Nüsslein-Volhard, C. and Jürgens, G. (1984). Mutations affecting the pattern of the larval cuticle in *Drosophila melanogaster*. III. Zygotic loci on the X-chromosome. *Wilhelm Roux's Arch. Dev. Biol.* **193**, 296-307.

White, K., Grether, M. E., Abrams, J. M., Young, L., Farrell, K. and Steller, H. (1994). Genetic control of programmed cell death in *Drosophila*. *Science* **264**, 677-683.

Yasuda, G. K., Baker, J. and Schubiger, G. (1991). Temporal regulation of gene expression in the blastoderm *Drosophila* embryo. *Genes Dev.* **5**, 1800-1812.